

Investigation of the Effects of Receptors on the Lightning Strike Protection of Wind Turbine Blades

Yeqing Wang and Weifei Hu

Abstract—Receptor plays an essential role in determining the efficiency of lightning strike protection (LSP) on wind turbine blades. To investigate the effects of receptors with different shapes and sizes on the LSP, we apply five different receptor configurations to the blade of a high-fidelity wind turbine model. The static electric field strength on the blade surfaces due to a lightning stepped leader is predicted through the development of a numerical model with finite element analysis. The interception efficiency is evaluated by comparing the predicted maximum electric field strength in the vicinity of the receptors. In addition, the locations of the predicted lightning strike attachment points match well with those obtained by experimental measurements, which validate the current numerical approach.

Index Terms—Finite element analysis (FEA), interception efficiency, lightning strike protection (LSP), receptor, wind turbine.

I. INTRODUCTION

LIGHTNING strike damage accounts for 23.4% of the wind turbine failure according to the 2012 US wind energy insurance claim report [1]. The repair of the lightning damage is often expensive and can lead to a significant amount of downtime. For example, 85% of the downtime is lightning related for a startup commercial wind farm at southwest of the USA, and the total lightning-related cost exceeded \$250 000 [2]. Lightning damage occurs to blades, generator, controller, control cables, etc. Among those, the blades are the most vulnerable components, which show the highest frequency (approximately 75%), highest repair cost, and longest downtime (approximately ten days per lightning incident) [3]. In addition, the increasing size of wind turbines in the recent years also poses significant challenges for the development of lightning strike protection (LSP) systems since the number of lightning strikes grows with the increase of structure height [4].

The most commonly used LSP system is to embed conductive (e.g., special tungsten alloy) receptors on the surfaces of wind turbine blades. These receptors are connected to down conductors (e.g., unshielded high-voltage cables), which are installed inside the blade shell extending from the root to the tip

of the blade. The receptors are designed to intercept the lightning strokes and safely conduct the lightning current through the down conductors to the earth. The efficiency of LSP is expressed as a product of interception efficiency and sizing efficiency, where the interception efficiency refers to the ability of the receptors to intercept a lightning stroke, and the sizing efficiency refers to the ability of the LSP system to conduct the lightning current [5]. The sizing efficiency can be increased by increasing the diameter of the down conductors. However, the interception efficiency is strongly dependent on the shape, size, quantity, and spacing of the receptors [5] and, therefore, requires a thorough investigation. Although, one receptor on each side of the blade tip is considered an adequate solution of LSP for blades shorter than 20 m [5], experiences have shown that lightning damages are still not avoidable [3]. Meanwhile, the shape and size of the receptors which play essential roles in determining the interception efficiency are not suggested in the current lightning protection standards [5] due to the lack of common practice of evaluating interception efficiency. Up to date, very few attempts have been undertaken to investigate the effects of shape and size of the receptors on the interception efficiency [6]. In particular, simulation studies related to this topic have rarely been reported. To come up with solutions to evaluate interception efficiency, a predictive model is proposed in this paper, and is applied to study the effects of the shape and size of the receptors on the interception efficiency.

In this paper, we apply receptors with different shapes and sizes on the blade tip to a high-fidelity wind turbine model. The static electric field strengths on the surfaces of the wind turbine blades due to a lightning stepped leader are obtained through the development of a numerical model with finite element analysis (FEA) that accounts for nonuniform charge density of the lightning stepped leader. The predicted location of the lightning strike attachment point on the blade surface is taken to be the location where the magnitude of electric field strength is the largest. In addition, the interception efficiency of the receptor is evaluated by comparing the corresponding maximum magnitudes of electric field strength on receptors with different shape and size configurations. In this paper, it is considered that the larger the electric field strength on the receptor, the higher possibility that the receptor intercepts the lightning stepped leader. In other words, the receptors with larger electric field strength provide better interception efficiency. The numerical approach is validated by qualitatively comparing the predicted lightning attachment locations on the blade surfaces with those obtained by experimental observations [6]. The results are of great

Manuscript received October 17, 2016; revised December 4, 2016; accepted December 29, 2016. Date of publication January 16, 2017; date of current version March 30, 2017.

Y. Wang is with the Department of Industrial and Systems Engineering, University of Florida, Research and Engineering Education Facility, Shalimar, FL 32579 USA (e-mail: yeqwang@reef.ufl.edu).

W. Hu is with the Department of Earth and Atmospheric Sciences, Cornell University, Ithaca, NY 14853 USA (e-mail: wh348@cornell.edu).

Color versions of one or more of the figures in this paper are available online at <http://ieeexplore.ieee.org>.

Digital Object Identifier 10.1109/TEMC.2016.2647260

importance in the future design and development of receptors for LSP systems on wind turbines.

II. PROBLEM FORMULATION

A. Lightning Stepped Leader Model

Large wind turbines with total height (one blade at its top vertical position) greater than 100 m experience both upward and downward lightning strikes [7]. Studies have shown that 50% of the lightning strikes on a 200-m-tall structure are upward initiated strikes [7]. Therefore, both upward and downward lightning strikes are quite common in wind turbines and are worth of consideration. However, upward lightning leader models have not been well established. In this paper, we focus on investigating the interaction between downward lightning strikes and wind turbines. A typical downward lightning discharge starts with a weakly luminous lightning stepped leader that originates from the columbium cloud and propagates through the air toward the ground structures. The electric field strength in the vicinity of the ground structures intensifies as the lightning stepped leader approaches which transport a large amount of electric charge. Answering leaders are emitted from the ground structures if the electric field gradient between the tip of the lightning stepped leader and the ground structure is sufficient to break down the air in between. If one of the answering leaders emitted from the ground structure arrests the lightning stepped leader, then the first luminous lightning return stroke is formed [8].

The lightning stepped leader model proposed by Cooray *et al.* [9] has been used in many recent simulation studies (e.g., [10] and [11]) for the prediction of electric fields induced by lightning strikes. In the model, the lightning stepped leader is idealized as a vertical line charge with nonuniform charge density

$$\begin{aligned} \lambda(\eta) = & a_0 \cdot \left(1 - \frac{\eta}{H - z_0}\right) \cdot G(z_0) \cdot I_{\text{peak}} \\ & + \frac{I_{\text{peak}} \cdot (a + b \cdot \eta)}{1 + c \cdot \eta + d \cdot \eta^2} \cdot F(z_0), \\ & 0 \leq \eta \leq L, \quad z_0 \geq 10 \end{aligned} \quad (1)$$

where $\lambda(\eta)$ is the charge density (in C/m); η (in m) is the distance from the tip of the leader and $\eta = z - z_0$; H is the height of the cloud (typically $H = 4000$ m); z_0 is the distance from the ground to the tip of the leader (in m); I_{peak} is the peak current of the return stroke (in kA); $G(z_0) = 1 - (z_0/H)$, $F(z_0) = 0.3\alpha + 0.7\beta$, $\alpha = \exp(-(z_0 - 10)/75)$, $\beta = 1 - (z_0/H)$, $a_0 = 1.476 \cdot 10^{-5}$, $a = 4.857 \cdot 10^{-5}$, $b = 3.9097 \cdot 10^{-6}$, $c = 0.522$, and $d = 3.73 \cdot 10^{-3}$. The charge density calculated by (1) shows favorable agreement with physical measurements as reported by Cooray *et al.* [9]. Thus, the lightning stepped leader model (1) with the above parameter values is used in this paper.

Based on the assumption that the horizontal extend of the negative charge region in the cloud is large in comparison to the vertical distance between the ground and the charge region, the cloud charge region can be replaced by a perfectly conductive plane maintained at a given cloud voltage [9]. The uniform background electric field between the cloud and the

ground is reported to be 10 kV/m [10], and the distance from the cloud to the ground is typically taken as 4000 m [9]–[11]. Therefore, the constant voltage $V = 40$ MV [10] is used in this paper. The ground is assumed as a conductive plane with zero electric potential.

The model [9] not only shows a good representation of the physics, but also allows to be easily incorporated into numerical analysis (e.g., FEA) due to the explicit expression of the charge density (1).

B. High-Fidelity Wind Turbine Models: Geometry and Setup

Traditional simulation studies related to the interaction of lightning strikes and wind turbine blades use simplified wind turbine geometries. For example, the wind turbine geometry including tower and blades is simplified as either straight lines or square beams [11]. However, a recent study [12] pointed out that when a tapered-beam-shaped (i.e., to capture the effects of pointer blade tip) wind turbine blade geometry is used, the electric field on the surface of the blade tip is about 18% larger than that when a constant cross-section beam-shaped wind turbine blade geometry is used.

In order to predict accurate electric fields, the National Renewable Energy Laboratory (NREL) 5-MW reference wind turbine [13] is adopted to develop the high-fidelity wind turbine model for lightning strike analysis. The geometries of the hub, nacelle, and tower of the wind turbine are modeled using the dimensions in the NREL reference wind turbine (see Figs. 1 and 2). As using a realistic blade geometry produces more accurate lightning-strike-induced electric fields than using simplified blade models (e.g., straight lines or square beams) [12], the NREL's blade geometry with 17 airfoils is further refined by adding additional 17 airfoils, which smooth the transition from section to section and create more realistic blade geometry [14], [15]. In this paper, the length of the blade, the radius of the hub, and the hub height are 60, 1.5, and 90 m, respectively. Thus, the maximum blade tip height when one of the blades is at its top vertical position is 151.5 m.

To investigate the effects of receptors, five different configurations of receptors (see Fig. 1) are applied on the wind turbine blade tip. Configuration 1 implements a raw blade with no receptors or down conductors; Configurations 2–5 apply receptors with different shapes (tip shape and disk shape) and sizes (lengths/radii) on blade tip as elaborated in Table I. Receptor distance from tip is also provided in Table I. All the receptors in configurations 2–5 are connected to the same down conductor inside the blade shell. Configurations 2–5 are chosen since the tip and disk shape receptors are the most widely used receptors on modern wind turbine blades, and multiple disk receptors are also widely used on blades longer than 20 m [5]. In addition, the experimental observations of lightning interception using the tip receptor, small disk receptor, and large disk receptor are available [6], which enabled us to compare our findings with the experimental observations.

In all cases considered in this paper, the three wind turbine blades are resting on the tower with one of the blades sits at its top vertical position, thus the dynamic effect of the blade

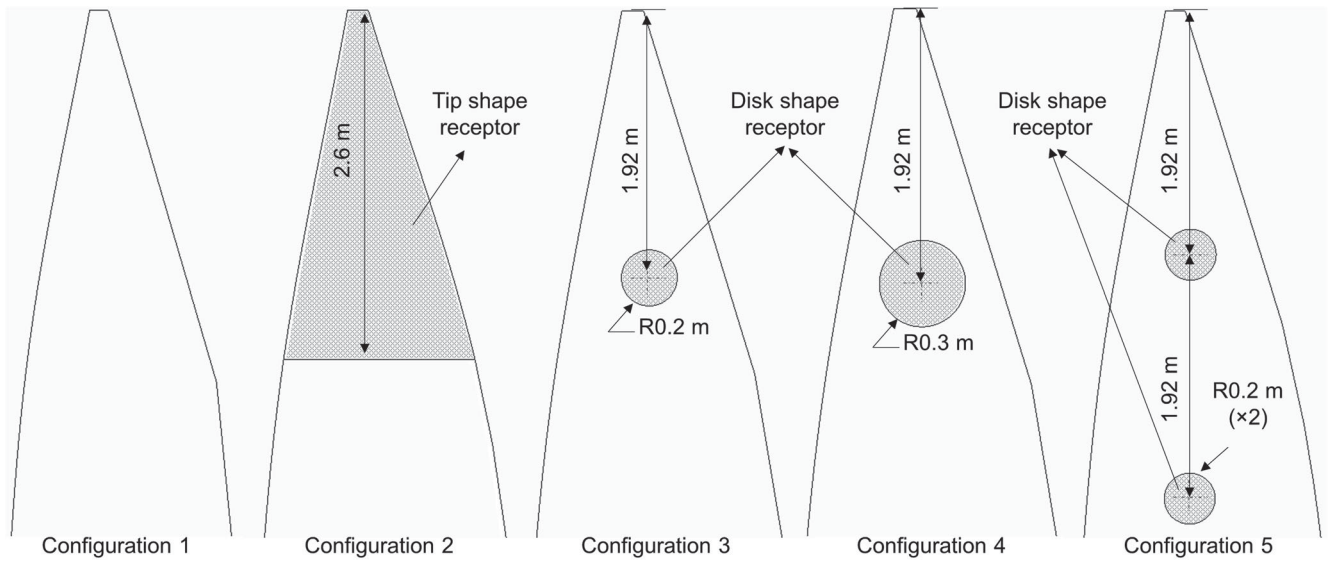


Fig. 1. Five different configurations of receptors used in the simulation study (size not to scale).

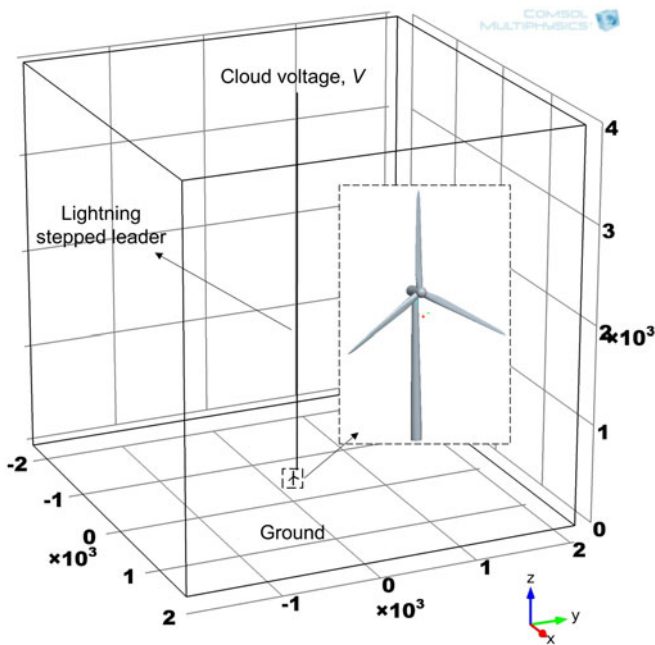


Fig. 2. Problem setup in COMSOL Multiphysics.

TABLE I
FIVE DIFFERENT RECEPTOR CONFIGURATIONS

Configurations	Receptor Characteristics
Configuration 1	No receptors or down conductors
Configuration 2	Tip shape receptor, length 2.6 m (extend from tip)
Configuration 3	Small disk shape receptor, radius 0.2 m, distance from tip 1.92 m
Configuration 4	Large disk shape receptor, radius 0.3 m, distance from tip 1.92 m
Configuration 5	Dual small disk shape receptor, radii 0.2 m, distance from tip to the first receptor 1.92 m, distance between the two receptors 1.92 m

rotation is not considered in this study. In addition, the effects of the dynamic propagation of the lightning stepped leader and the answering leader on the predicted electric field are also not considered. These dynamic effects lead to moving boundary conditions to the current problem, which requires a completely different approach of analysis. Such analysis is beyond the scope of this paper. In this paper, we focus on evaluating the interception efficiency of various receptors by checking the maximum static electric field strength induced by the lightning stepped leader at the particular moment when the leader arrives within the lightning striking distance.

The lightning striking distance between the lightning stepped leader and the wind turbine is calculated using the rolling sphere method [7], [9], [16],

$$R = 0.6 \cdot I_{\text{peak}}^{1.46} \quad (2)$$

where R is the lightning striking distance (in m) and I_{peak} is the peak current (in kA). As suggested by the lightning protection standard [5], it is appropriate to use the rolling sphere method for the current wind turbine model with blade length longer than 20 m. In addition, the rolling sphere is assumed to be tangentially attached to the tip of the top-vertically-positioned blade.

According to Gameraota *et al.* 50% of the measured negative first return strokes reach a peak current of 30 kA [17]. Therefore, in this study, the peak current I_{peak} used in all the simulations are chosen as 30 kA to represent the general situation of lightning strikes.

III. NUMERICAL IMPLEMENTATION

Static electric fields in the vicinity of the wind turbines with blade models of different receptor configurations due to the lightning stepped leader are solved using FEA. The governing equations of the problem and the corresponding numerical setup and implementation are discussed in this section.

A. Governing Equations

The electric field due to a given vertically charged lightning stepped leader can be calculated using the equations of electrostatics

$$\nabla \times \mathbf{E} = 0, \quad (3)$$

$$\nabla \cdot \mathbf{E} = \rho_v / \epsilon_0, \quad (4)$$

$$\mathbf{E} = -\nabla \phi \quad (5)$$

where \mathbf{E} denotes the electric field tensor, ρ_v is the source of electric charge, $\rho_v = \lambda / \pi r^2$, where λ is the line charge density (1), r is the radius of the vertical cylindrical lightning stepped leader channel, $r = 1.5$ m, ϵ_0 is the permittivity of the free space, and ϕ is the electric potential.

It should be noted that the lightning striking distance (2) determines the relative spatial position between the lightning stepped leader and the wind turbine geometry in the computational domain, and also determines the locations of the zero electric potential boundary conditions that are associated with the surfaces of the conductive receptors, hub, nacelle, and the tower.

B. Numerical Implementation

The FEA software COMSOL Multiphysics is used to solve the governing equations (3)–(5). The computational domain is $4000 \text{ m} \times 4000 \text{ m} \times 4000 \text{ m}$ with a cutout of the developed high-fidelity wind turbine model as shown in Fig. 2. The wind turbine cutout is located on the ground. The lightning stepped leader is located at the center of the domain extending from the top surface to 151.5 m (i.e., the maximum blade tip height of the wind turbine) above the ground (i.e., bottom surface of the computational domain). The distance between the lightning stepped leader and the wind turbine cutout is calculated by (2).

The four vertical side surfaces of the entire computational domain are applied with open boundary condition. In addition, the surfaces on the hub, nacelle, and tower of the wind turbine geometry are applied with ground potential, since the materials used on these components are typically steel and aluminum [18], which are electrically conductive. To account for the effect of receptors, a ground potential is also applied to the surfaces of the tip receptor used in configuration 2, and the disk receptors used in configurations 3–5. The remaining surface of the wind turbine blade is applied with open boundary conditions since the remaining surface of the blade is made of electrically non-conductive materials (i.e., nonconductive laminated glass fiber composite fabrics and nonconductive surface finish).

The computational domain and the lightning stepped leader are assigned with “air” material as defined in the COMSOL material library. The top surface of the domain is applied with a cloud voltage, $V = 40 \text{ MV}$ [10]. The computational domain is meshed with 1 892 940 (averaged number for all the simulation cases) free tetrahedral elements. The minimum and maximum element sizes are 0.5 and 100 m, respectively. The maximum element growth rate is 1.3, and the resolution of curvature and narrow regions are 0.5 and 0.9, respectively. In order to balance computational efficiency and accuracy, the meshes nearby

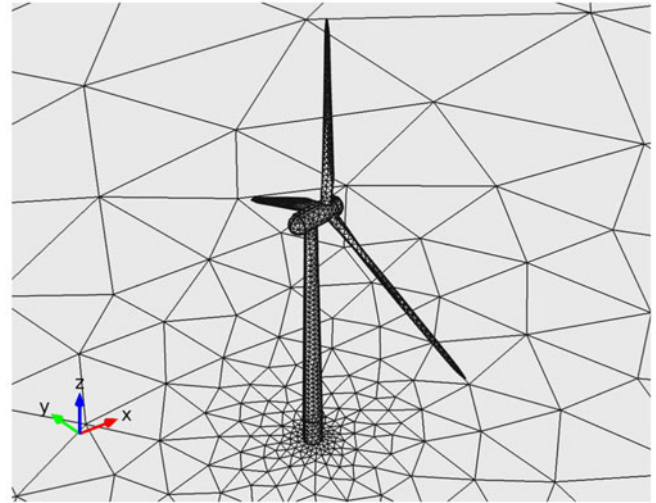


Fig. 3. Surface mesh associated with the high-fidelity wind turbine model.

the turbine are refined and more coarse meshes are used away from the turbine. An example of surface mesh associated with the wind turbine is shown in Fig. 3. Although it appears that the maximum element size, 100 m, is comparatively large to achieve an accurate prediction of the electric field distribution. Our investigation (see Section IV) shows that the maximum element size 100 m is sufficiently small for the current simulation study. Meanwhile, reducing the maximum element size will lead to a significant increase in the number of elements, which requires substantial computational memory. Under our current computational capability using a four-core laptop with 4-GB RAM, 100 m was tested to be the smallest maximum element size for the simulation to be successfully implemented. If a large workstation is available, a finer mesh can be implemented to achieve much higher accuracy. The averaged computational time for studying each receptor configuration under current computational capability is 1200 s.

IV. RESULTS AND DISCUSSIONS

In this section, the predicted electric field strengths on the surfaces of the blade using five receptor configurations (see Table I) are presented. Note that only the results for the blade at its top vertical position are discussed in this section since the corresponding electric field strengths are much higher than those on the surfaces of the other two blades. The locations of the blade surfaces with higher electric field strength are considered to have higher possibility of emitting answering leaders and arresting the lightning stepped leader.

First, the dependence of the electric field strength on the maximum element size is investigated. Figure 4 shows the comparisons of the predicted electric field strength distribution at the tip region of the blade (configuration 4) obtained when the maximum element size in the simulation is set to 400 [see Fig. 4(a)], 300 [see Fig. 4(b)], 200 [see Fig. 4(c)], and 100 m [see Fig. 4(d)], respectively. As shown in Fig. 4, the predicted maximum electric field strengths using the four different maximum

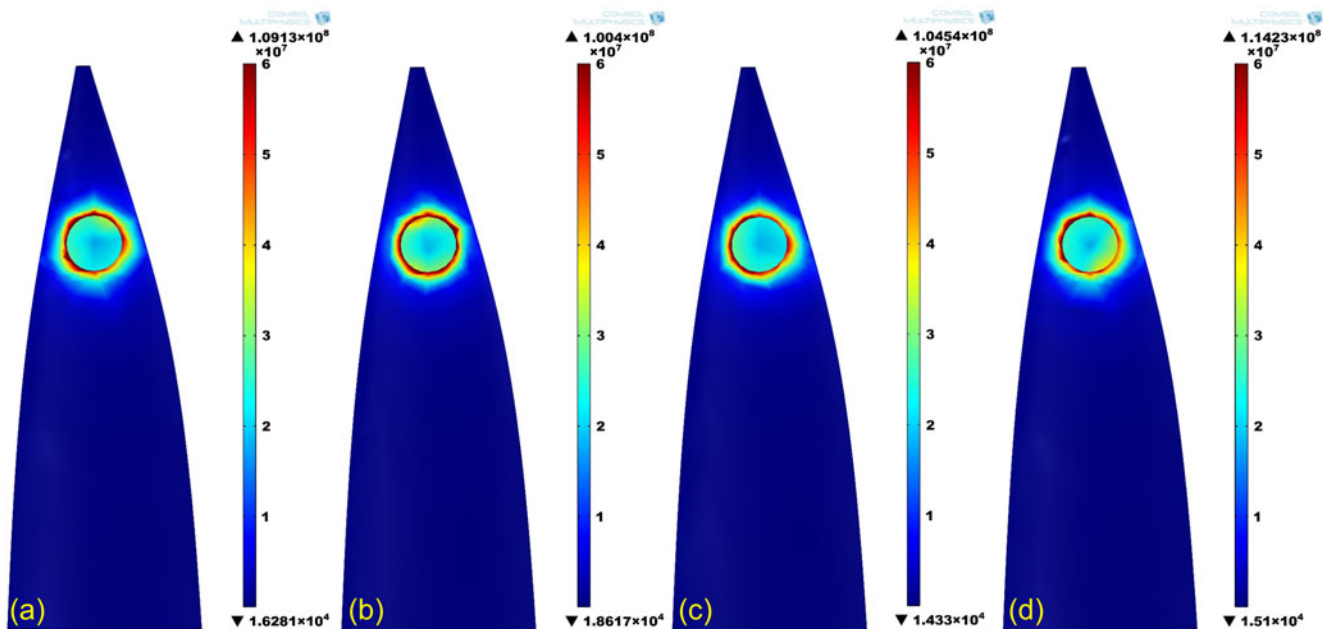


Fig. 4. Effects of maximum mesh size on the predicted electric field strength distributions at the tip regions (Configuration 4): (a) maximum mesh size equals 400 m; (b) maximum mesh size equals 300 m; (c) maximum mesh size equals 200 m; and (d) maximum mesh size equals 100 m.

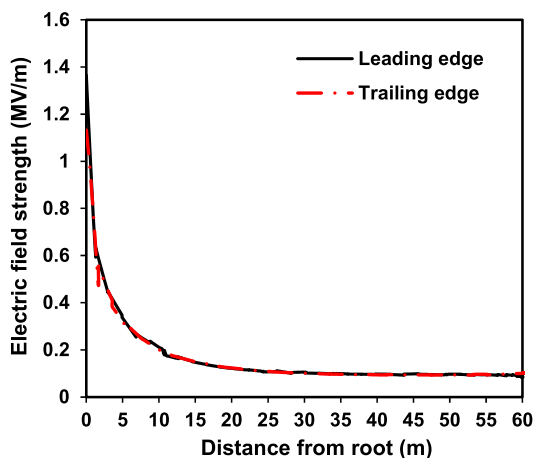


Fig. 5. Predicted electric field strength along the trailing and leading edges of the wind turbine blade model with no receptors or down conductors.

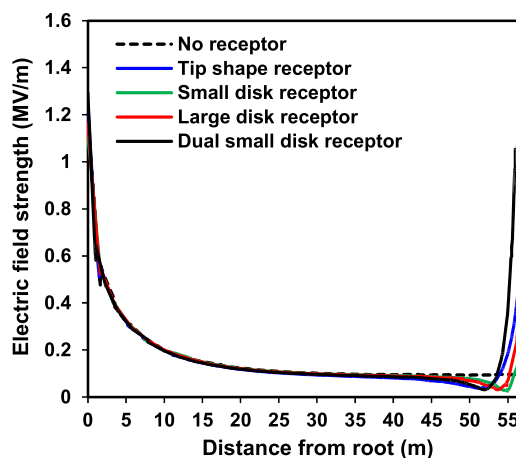


Fig. 6. Comparison of predicted electric field strength along the trailing edge in the range of 0–57 m from the root for different receptor configurations.

element mesh sizes are in the same order of magnitude, while using the maximum mesh size of 100 m produces the most conservative predicted electric field strength. Therefore, to achieve a conservative prediction, all the simulation results are obtained using a maximum element size of 100 m in the following paper.

Figure 5 shows the electric field strength along the trailing and leading edge of the wind turbine blade with no receptors or down conductors (configuration 1). There is no significant difference of electric field strength along the trailing and leading edge when no receptors or down conductors are installed. Figure 6 shows the comparison of electric field strengths along the trailing edge in the range of 0–57 m from root for the five different receptor configurations. It can be seen that the electric field strengths for different receptor configurations are identical

within 0–50 m from the root. However, a significant increase of electric field strength can be observed near the blade tip regions where receptors are installed comparing to the case in which no receptor is installed. In order to further investigate the electric field at the tip region, Fig. 7 shows the corresponding predicted electric field strengths along the trailing edge at the tip regions (i.e., 57–60 m from root) of the blade models with receptors. Comparing Figs. 6 and 7, it can be noticed that the electric field strength at the tip region is about two to three orders higher than that at the inboard region for the cases in which receptors are installed. In contrast, the electric field strength for the blade without receptors or down conductors remains low at the tip region (see Fig. 6). The same trend can be found for the predicted electric field strengths along the leading edge, shown in Figs. 8

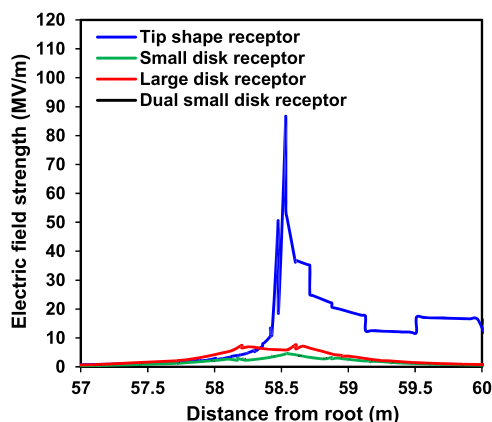


Fig. 7. Comparison of predicted electric field strength along the trailing edge at the tip region for different receptor configurations.

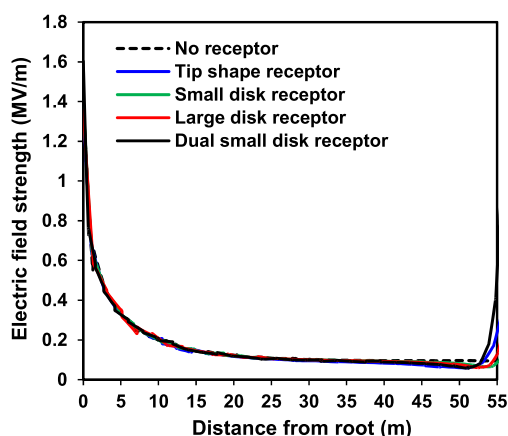


Fig. 8. Comparison of predicted electric field strength along the leading edge in the range of 0–55 m from the root for different receptor configurations.

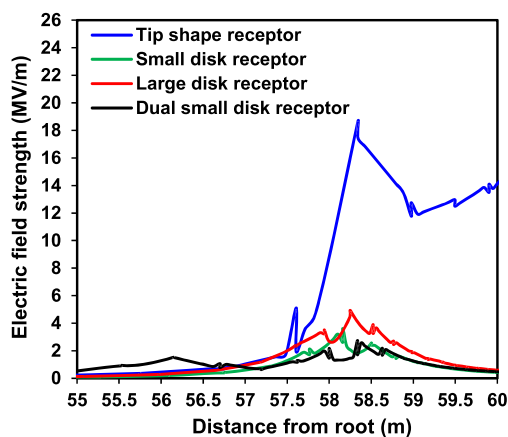


Fig. 9. Comparison of predicted electric field strength along the leading edge at the tip region for different receptor configurations.

and 9. These results indicate that the presence of these receptors greatly enhances the electric field. Therefore, answering leaders are more likely to be emitted from those receptors than from the insulated area of the blade surface. In this way, lightning current is safely conducted through the conductive receptor and internal down conductors without producing extensive lightning damages on the insulated areas of the wind turbine blades. In

this paper, the lightning attachment point on the blade surface is chosen at the location, where the magnitude of electric field strength is largest.

It should be mentioned that although the electric field strength of the wind turbine blade model without receptors is low comparing to those of the wind turbine blade models with receptors, it does not mean that answering leaders will not be emitted from the blade surface. In real situations, lightning strike often comes with heavy rains. The electrically conductive rain droplets attached on the blade surface may also enhance the local electric field strength and therefore trigger answering leaders. If lightning strike injects directly into the blade surface, the associated high-intensity heat flux (approximately 10^9 W/m²) may lead to considerable damages, including delamination of the laminated composite blade structure, debonding of shells, thermal ablation, and even explosion [19], [20].

A close examination of results in Figs. 7 and 9 reveals that the electric field strengths on the trailing and leading edges are much higher when the tip shape receptor is used than those when disk shape receptors are used. This is because the trailing and leading edges of the blade models using disk receptors are still nonconductive, whereas the trailing and leading edges of the blade models using tip shape receptor is electrically conductive. In addition, the maximum electric field strengths along the trailing edge (see Fig. 7) and along the leading edge (see Fig. 9) using the large disk shape receptor are around 1.5–2 times higher than those using the small disk shape receptor. This is due to the closer distance between the blade edges (trailing and leading edges) and the circumference of the conductive receptors when larger diameter disk is used. Figure 9 also shows two peaks (approximately 56.2 and 58.3 m from the root) with high electric field strength when the dual small disk receptor blade model is used. The peak close to the tip is higher than the one further away from the tip, which implies that the disk receptor close to the tip may have comparably higher chances of emitting answering leaders. It should be noted that Figs. 7 and 9 show only the maximum electric field strength on the trailing and leading edges of the blade. The maximum electric field strength on the surface of the entire tip region can be found by plotting the electric field strength distributions as shown in Fig. 10.

The predicted electric field strength distributions on the surfaces of the tip regions of the wind turbine blade with receptor configurations 2–5 are provided in Fig. 10(a)–(d), respectively. Meanwhile, the experimental measurements of lightning strike attachments on real 3-m partial blade models with tip shape receptor, small disk receptor, and large disk receptors reported by Arinaga *et al.* [6] are shown in Fig. 10(e)–(g), respectively. Although the length of the blade and the size of the receptors used in the experimental measurements are different from those used in our simulation, the experimental results provide some qualitative insight into the influence of shape and size of the receptors, and therefore are used to check the effectiveness of our numerical model.

It can be noticed that the maximum electric field strength on the surface of the blade model with tip shape receptor is located at the interface between the tip receptor and the rest of the blade

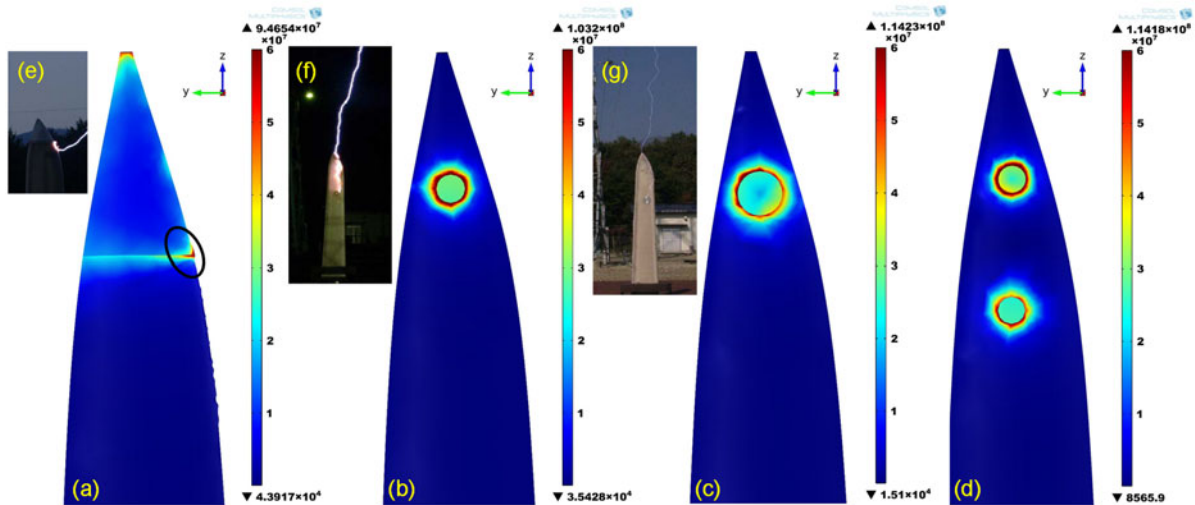


Fig. 10. Comparison of predicted electric field strength distributions at the tip regions for different receptor configurations: (a) tip shape receptor; (b) small disk shape receptor; (c) large disk shape receptor; (d) dual small disk shape receptor; (e) experimental result for tip shape receptor [6]; (f) experimental result for small disk shape receptor [6]; and (g) experimental result for large disk shape receptor [6].

TABLE II
MAXIMUM PREDICTED ELECTRIC FIELD STRENGTH AND LOCATIONS

Receptor Configurations	Max. Electric Field Strength (MV/m)	Locations of Max. Electric Field Strength
Configuration 2	94.65	Interface between tip receptor and blade on the trailing edge
Configuration 3	103.20	Adjacent outer boundaries of circumference of the disk receptor
Configuration 4	114.23	Adjacent outer boundaries of circumference of the disk receptor
Configuration 5	114.18	Adjacent outer boundaries of circumference of the first disk receptor

on the trailing edge [see Fig. 10(a)], which implies that the answering leaders will most likely be emitted from this location. This location finding agrees favorably well with the experimental measurement shown in Fig. 10(e), in which we can notice that the lightning attaches to the exact same location of the blade. In addition, Fig. 10(b)–(d) reveal that the maximum electric field strengths are not located on the receptors themselves. Instead, they are located at the outer boundaries adjacent to the circumference of the disk receptors. And these are the most possible locations for lightning strike attachments. These location predictions also compare well with the experimental measurements shown in Fig. 10(f) and (g), in which it can be observed that lightning strikes attach to the same locations as we predicted. This finding also explains that many of real blades exhibited little holes near the receptors after lightning strikes [3]. No experimental measurement is available for the case using the dual small disk shape receptor.

The predicted maximum electric field strength and their corresponding locations on the surface of the blade model using receptors are listed in Table II. It is found that the blade using the large disk receptor presents the highest electric field strength, whereas the maximum electric field strength on the blade with the tip shape receptor is the lowest among all of the four configurations. This indicates that disk shape receptors

provide higher interception efficiency than tip shape receptors do, and using disk shape receptors is more desirable. In addition, it is found that the maximum electric field strength of the blade with large disk receptor is 10.69% higher than that of the blade with small disk receptor, which indicates that increasing the size of the disk shape receptor may lead to an increase in the interception efficiency. Furthermore, the maximum electric field strength of the blade model using dual small disk shape receptor is 10.64% higher than that of the blade model using a single small disk shape receptor. In addition, the dual small disk shape receptor also allows more chances of emitting answering leader thus would be more favorable for longer blades. However, increasing the size of the disk receptor and adding more disk receptors would adversely increase weight of the blade, and therefore may increase the cost and compromise the mechanical performance.

The aforesaid findings could also be extendable to a different size turbine if receptor configurations (see Table I) are proportionally scaled based on the length ratio between the investigated blade used in this paper and the blade from the different size turbine. Under such condition, the relative location of the receptors (i.e., and therefore the zero electric potential boundary condition) from the blade tip, leading and trailing edges are also scaled. Therefore, given a fixed lightning current, and thus fixed lightning striking distance and charge density [ρ_v in (4)], the predicted electric field on a different size turbine will also be scaled from those predicted under the current blade and receptor configurations. Although the exact values of the predicted electric field strength on a different size turbine will be different due to the shift of the zero electric potential boundary conditions, the ratios between the predicted electric field strengths on the different size blade using scaled five receptor configurations are identical with those obtained under the current blade and receptor configurations. Therefore, the conclusions in the current study about the comparisons of the interception efficiency of the five receptor configurations still hold.

V. CONCLUSION

In this paper, the effects of receptors on the LSP of wind turbine blades have been investigated. The static electric field strength on the blade surface of a high-fidelity 5-MW NREL reference wind turbine model has been predicted through the development of a numerical model using FEA. The nonuniform charge density of the lightning stepped leader has been incorporated in the numerical model. The interception efficiency of the receptors with different shape and size configurations has been evaluated by comparing the predicted maximum electric field strength on the surfaces of the tip regions. The effectiveness of the numerical model has been validated by qualitatively comparing the predicted lightning attachment locations with the existing experimental observations. Our results show that the disk shape receptor presents more favorable interception efficiency than the tip shape receptor does. In addition, increasing the size of the disk receptor and using dual disk receptors may also increase the interception efficiency. However, the additional weight could lead to an increase of cost and a possible compromise of mechanical performance. Note that the results from the current numerical model will necessarily depend on the adopted lightning striking distance model and on the appropriate choice of the simulation parameters such as the minimum and maximum mesh sizes, and the element growth rate.

The current proposed approach of evaluating the interception efficiency of the receptors can also be adopted to facilitate the design and development of advanced lightning receptors by optimizing the configurations, such as the shape, size, pattern, and location.

It is also worth mentioning that, in addition to the receptors, the insulation or shielding of the conductive components inside the blades (e.g., receptor holder, down conductors) also has a significant impact on the interception efficiency [19]. The investigation of these effects requires a separate analysis that is capable of capturing the electric field distributions inside the blade structure, and is a subject of our future research.

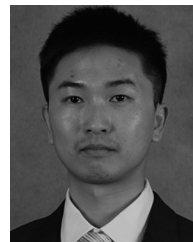
ACKNOWLEDGMENT

The authors gratefully acknowledge the courtesy of the lightning strike experimental photos which are provided by S. Arinaga, K. Inoue, and T. Matsushita, as the validation of the simulated analysis results.

REFERENCES

- [1] Gcube-insurance. GCube top 5 US wind energy insurance claims report. 2012. [Online]. Available: <http://www.gcube-insurance.com/en/press/gcube-top-5-us-wind-energy-insurance-claims-report/>
- [2] R. Kithil, "Lightning hazard reduction at wind farms," American Wind Energy Assoc., Washington, DC, USA, 1997.
- [3] H. Braam, "Lightning damage of owecs, Part 1: Parameters relevant for cost modelling," ECN-C-02-053, Jun. 2002.
- [4] R. Beckers, Lightning Protection, 2016. [Online]. Available: <http://www.solacity.com/lightning-protection/>
- [5] IEC, 61400-24 Wind turbine generator systems—Part 24: Lightning protection, IEC, Geneva, Switzerland, 2002.
- [6] S. Arinaga, K. Inoue, and T. Matsushita, "Experimental study for wind turbine blades lightning protection," presented at the Renewable Energy Int. Conf., 2006.

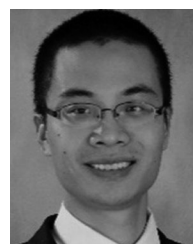
- [7] V. Rakov, "The physics of lightning," *Surveys Geophys.*, vol. 34, pp. 701–729, 2013.
- [8] V. A. Rakov and M. A. Uman, *Lightning: Physics and Effects*: Cambridge, U.K.: Cambridge Univ., 2003.
- [9] V. Cooray, V. Rakov, and N. Theethayi, "The lightning striking distance—Revisited," *J. Electrostatist.*, vol. 65, pp. 296–306, 2007.
- [10] M. Becerra, "On the attachment of lightning flashes to grounded structures," Ph.D. dissertation, Uppsala Univ., Uppsala, Sweden, 2008.
- [11] B. Lewke, Y. M. Hernández, and J. Kindersberger, "A simulation method for the wind turbine's electric field distribution caused by the stepped lightning leader," in *Proc. Eur. Wind Energy Conf.*, Milan, Italy, 2007, pp. 1345–1349.
- [12] Y. Wang and O. I. Zhupanska, "Estimation of the electric fields and dielectric breakdown in non-conductive wind turbine blades subjected to a lightning stepped leader," *Wind Energy*, Nov. 4, 2016. [Online], DOI: 10.1002/we.2071.
- [13] J. Jonkman, S. Butterfield, W. Musial, and G. Scott, "Definition of a 5-MW reference wind turbine for offshore system development," National Renewable Energy Laboratory, Golden, CO, USA, 2009.
- [14] W. Hu, K. Choi, O. Zhupanska, and J. H. Buchholz, "Integrating variable wind load, aerodynamic, and structural analyses towards accurate fatigue life prediction in composite wind turbine blades," *Struct. Multidisciplinary Optimization*, vol. 53, pp. 375–394, 2016.
- [15] W. Hu, K. K. Choi, and H. Cho, "Reliability-based design optimization of wind turbine blades for fatigue life under dynamic wind load uncertainty," *Struct. Multidisciplinary Opt.*, vol. 54, pp. 953–970, 2016.
- [16] A. J. Eriksson, "The lightning ground flash: An engineering study," Ph.D. dissertation, Univ. Natal, Durban, South Africa, 1980.
- [17] W. R. Gameraota, J. O. Elisimé, M. A. Uman, and V. A. Rakov, "Current waveforms for lightning simulation," *IEEE Trans. Electromagn. Compat.*, vol. 54, no. 4, pp. 880–888, Aug. 2012.
- [18] D. Ancona and J. McVeigh, "Wind turbine-materials and manufacturing fact sheet," Princeton Energy Resources Int., LLC, vol. 19, 2001.
- [19] A. C. Garolera, S. F. Madsen, M. Nissim, J. Myers, and J. Holboell, "Lightning damage to wind turbine blades from wind farms in US," *IEEE Trans. Power Del.*, vol. 31, no. 3, pp. 1043–1049, Jun. 2016.
- [20] Y. Wang and O. Zhupanska, "Lightning strike thermal damage model for glass fiber reinforced polymer matrix composites and its application to wind turbine blades," *Composite Struct.*, vol. 132, pp. 1182–1191, 2015.



Yeqing Wang received the B.Eng. degree in vehicle engineering in 2009 from Southwest Jiaotong University, Chengdu, China, and the Master's and Ph.D. degrees in mechanical engineering in 2016 from the University of Iowa, Iowa City, IA, USA.

He is currently a Postdoctoral Research Associate with the Department of Industrial and System Engineering at the University of Florida, Gainesville, FL, USA. His research interests include multiphysics problems, thermal ablation problems, wind energy, and finite element analysis.

Dr. Wang received the Best Paper Award at the 2012 American Society for Composites Technical Conference.



Weifei Hu received the B.S. degree in 2008 from Zhejiang University, Hangzhou, China, the M.S. degree in 2010 from Hanyang University, Seoul, South Korea, and the Ph.D. degree in 2015 from the University of Iowa, Iowa city, IA, USA, all in mechanical engineering.

He is currently a Postdoctoral Research Associate at Cornell University, Ithaca, NY, USA. He is interested in a wide range of wind energy topics including wind turbine aerodynamics and structure, wind turbine composite materials, wind turbine lightning strike protection, wind gust detection, wind turbine condition monitoring, and reliability-based design optimization (RBDO) of wind turbine systems. His work has been published in peer-reviewed journals and conference proceedings, e.g., the *Journal of Structural and Multidisciplinary Optimization*, *Journal of Mechanical Science and Technology*, and ASME and AIAA proceedings. His journal paper (first author) on RBDO of wind turbine blades is featured by Renewable Energy Global Innovations.

Dr. Hu is a Technical Committee Member and the Secretary (2016–2017) of the Renewable and Advanced Energy Systems Committee in the Power Division of ASME.